9-17-2022

Cytogenetic and genomic characterization of a novel tall wheatgrass-derived *Fhb7* allele integrated into wheat B genome

Wei Zhang
Shanxi Agricultural University, North Dakota State University

Tatiana Danilova
USDA-ARS

Mingyi Zhang
North Dakota State University

Shuangfeng Ren
North Dakota State University

Xianwen Zhu
North Dakota State University

See next page for additional authors

Theoretical and Applied Genetics
https://doi.org/10.1007/s00122-022-04228-3

ORIGINAL ARTICLE

Cytogenetic and genomic characterization of a novel tall wheatgrass-derived *Fhb7* allele integrated into wheat B genome

Wei Zhang[1,2] · Tatiana Danilova[3] · Mingyi Zhang[2] · Shuangfeng Ren[2] · Xianwen Zhu[2] · Qijun Zhang[2] · Shaobin Zhong[4] · Linda Dykes[5] · Jason Fiedler[5] · Steven Xu[6] · Katherine Frels[7] · Stephen Wegulo[8] · Jeffrey Boehm Jr.[3,7] · Xiwen Cai[3,7]

Received: 15 August 2022 / Accepted: 17 September 2022

Abstract

Key message **We identified and integrated the novel FHB-resistant *Fhb7*^{The2} allele into wheat B genome and made it usable in both common and durum wheat breeding programs without yellow flour linkage drag.**

Abstract A novel tall wheatgrass-derived (*Thinopyrum elongatum*, genome EE) *Fhb7* allele, designated *Fhb7*^{The2}, was identified and integrated into the wheat B genome through a small 7B–7E translocation (7BS·7BL–7EL) involving the terminal regions of the long arms. *Fhb7*^{The2} conditions significant Type II resistance to Fusarium head blight (FHB) in wheat. Integration of *Fhb7*^{The2} into the wheat B genome makes this wild species-derived FHB resistance gene usable for breeding in both common and durum wheat. By contrast, other *Fhb7* introgression lines involving wheat chromosome 7D can be utilized only in common wheat breeding programs, not in durum wheat. Additionally, we found that *Fhb7*^{The2} does not have the linkage drag of the yellow flour pigment gene that is tightly linked to the decaploid *Th. ponticum*-derived *Fhb7* allele *Fhb7*^{Thp}. This will further improve the utility of *Fhb7*^{The2} in wheat breeding. DNA sequence analysis identified 12 single nucleotide polymorphisms (SNPs) in *Fhb7*^{The2}, *Fhb7*^{Thp}, and another *Th. elongatum*-derived *Fhb7* allele *Fhb7*^{The1}, which led to seven amino acid conversions in Fhb7^{The2}, Fhb7^{Thp}, and Fhb7^{The1}, respectively. However, no significant variation was observed in their predicted protein configuration as a glutathione transferase. Diagnostic DNA markers were developed specifically for *Fhb7*^{The2}. The 7EL segment containing *Fhb7*^{The2} in the translocation chromosome 7BS·7BL–7EL exhibited a monogenic inheritance pattern in the wheat genetic background. This will enhance the efficacy of marker-assisted selection for *Fhb7*^{The2} introgression, pyramiding, and deployment in wheat germplasm and varieties.

Introduction

Fusarium head blight (FHB), caused primarily by the fungus *Fusarium graminearum*, is a devastating disease of wheat worldwide. Host resistance has been considered the most effective tactic in managing this disease to reduce the

Communicated by Lingrang Kong.

Wei Zhang and Tatiana Danilova have contributed to this work equally.

✉ Xiwen Cai
xiwen.cai@usda.gov

1 Shanxi Key Laboratory of Minor Crop Germplasm Innovation and Molecular Breeding, Shanxi Agricultural University, Taiyuan 030031, China

2 Departments of Plant Sciences, North Dakota State University, Fargo, ND 58108, USA

3 Wheat, Sorghum & Forage Research Unit, USDA-ARS, Lincoln, NE 68583, USA

4 Department of Plant Pathology, North Dakota State University, Fargo, ND 58108, USA

5 Cereal Crops Research Unit, Edward T. Schafer Agricultural Research Center, USDA-ARS, Fargo, ND 58102, USA

6 Crop Improvement and Genetics Research Unit, Western Regional Research Center, USDA-ARS, Albany, CA 94710, USA

7 Department of Agronomy and Horticulture, University of Nebraska, Lincoln, NE 68583, USA

8 Department of Plant Pathology, University of Nebraska, Lincoln, NE 68583, USA

Published online: 06 October 2022

economic losses in the wheat production and food industries (Wilson et al. 2017). A Chinese common wheat variety, 'Sumai 3', has long been a primary source of FHB resistance that is widely deployed in many wheat varieties around the world, resulting in a narrow genetic basis of FHB resistance in wheat. Native resistance to FHB remains limited in all market classes of wheat, especially in durum wheat (Haile et al. 2019). The search for new FHB resistance genes from wheat-related wild grasses has increasingly received special attention of wheat researchers to diversify and enhance the resistance of wheat to FHB (Cai et al. 2005; Oliver et al. 2008; Zhang and Cai 2019; Wang et al. 2020).

Resistance to FHB has been identified in the relatives of wheat, including wild and domesticated species (Shen et al. 2004; Cai et al. 2005; Oliver et al. 2007, 2008; McArthur et al. 2012; Zhang et al. 2014; Szabó-Hevér et al. 2018). Some of the resistance sources have been incorporated into wheat by chromosome engineering and mapped in the wheat genome using DNA markers (Otto et al. 2002; Buerstmayr et al. 2003; Chen et al. 2007; Qi et al. 2008; Zhang et al. 2011; Cainong et al. 2015; Zhu et al. 2016; Wang et al. 2020). They represent an invaluable gene pool of breeding for FHB resistance in wheat.

The advances in genomics and high-throughput genotyping have dramatically improved the efficacy and throughput of the meiotic homoeologous recombination-mediated chromosome engineering in the alien introgression and genome study of wheat and its relatives (Niu et al. 2011; Zhang et al. 2017; Zhang et al. 2018; Grewal et al. 2020; Zhang et al. 2020). This has provided new opportunities to exploit wild species for novel FHB resistance genes and to bridge the gene flow from wild species into wheat. Several wild species-derived FHB resistance genes, including *Fhb3*, *Fhb6*, and *Fhb7*, have been identified, mapped, and incorporated into the wheat genome by chromosome engineering (Shen et al. 2004; Oliver et al. 2008; Qi et al. 2008; Zhang et al. 2011; Cainong et al. 2015; Guo et al. 2015). More recently, *Fhb7* was cloned from decaploid tall wheatgrass *Thinopyrum ponticum* ($2n = 10x = 70$) that shares the E genome with the diploid tall wheatgrass species *Th. elongatum* ($2n = 2x = 14$, genome EE) based on the reference genome of *Th. elongatum*. *Fhb7* was found to confer Type II FHB resistance and to detoxify *Fusarium*-produced trichothecenes, such as deoxynivalenol (DON), in wheat (Wang et al. 2020). Several *Fhb7* resistance alleles have been integrated into the wheat D genome through 7D–7E translocation from *Th. elongatum* and *Th. ponticum*, respectively (Guo et al. 2015; Fedak et al. 2021; Ceoloni et al. 2017). Also, research effort has been made to transfer *Th. ponticum*-derived *Fhb7* resistance allele to the wheat A genome through 7A–7E translocation (Forte et al. 2014). The present study identified and characterized a novel FHB-resistant *Fhb7* allele derived from *Th. elongatum* by molecular cytogenetic and genomic analyses. In addition, we incorporated this novel *Fhb7* allele into the wheat B genome by meiotic homoeologous recombination-based chromosome engineering, making this novel FHB resistance allele usable in common and durum wheat breeding programs.

Materials and methods

Plant materials

Common wheat 'Chinese Spring' (CS) -*Th. elongatum* disomic substitution line 7E(7B) [DS 7E(7B)], supplied by J. Dvorak at University of California (Davis, USA), was identified resistant to FHB in our previous study (Oliver et al. 2008). It was utilized as the initial FHB-resistant material to induce meiotic homoeologous recombination between wheat chromosome 7B and *Th. elongatum* chromosome 7E as described by Zhang et al. (2020). The 7B–7E recombinants involving the long arm of chromosome 7E possessing the *Fhb7* locus (Wang et al. 2020; Zhang et al. 2020) were evaluated for reaction to FHB pathogen. One of the FHB-resistant 7B–7E recombinants with the smallest 7EL segment was used in this study. It was selected from the 7B–7E recombination population produced by crossing DS 7E(7B) to CS *ph1b* mutant and backcrossing to CS *ph1b* mutant as described by Zhang et al. (2020). The wheat-*Th. ponticum* translocation line 'KS10-2', which contains the *PSY-E1* gene for yellow flour color on the translocation chromosome 7DS-7el$_2$S·7el$_2$L (Kim et al. 1993; Zhang et al. 2005; Zhang and Dubcovsky 2008; Niu et al. 2014), was used as positive control in the genetic analysis of the yellow flour pigment gene.

FHB disease evaluation and data analysis

The critical 7B–7E recombinants and their parents were evaluated for FHB resistance by the point inoculation method in the greenhouse as described by Zhu et al. (2016). At least eight plants grown in four pots were included in the disease evaluation experiment for each genotype. The infected spikelets in a spike were scored at 21 days post-inoculation, and FHB severity was calculated as the percentage of infected spikelets in over 40 inoculated spikes for each genotype. ANOVA was performed on FHB severity of the 7B–7E recombinants and their parents. Fisher's protected LSD was used for mean separation between the genotypes. All statistical analyses were conducted using R version 4.1.0.

Molecular cytogenetic analysis

Chromosome preparation, probe labeling, and the fluorescent in situ hybridization (FISH) were performed according to Kato et al. (2004, 2006) with minor modifications (Danilova et al. 2012). The tandem repeat *pSc119-2* (McIntyre et al. 1990) and microsatellite $(GAA)_n$ were used to identify wheat chromosomes and verify the structure of recombinant chromosomes. The FISH probe mixture (10 µl/slide) in 2 × SSC-1 × TE buffer contained 150 ng of E genome-specific probe (Danilova et al., unpublished) labeled with fluorescein-12-dUTP (PerkinElmer, Waltham, MA, USA), 5 ng of oligonucleotide probe $Cy5\text{-}(GAA)_9$ (synthesized by Integrated DNA Technologies, Inc., Coralville, IA, USA), 40 ng of *pSc119-2* probe labeled with Texas red-5-dCTP (PerkinElmer, Waltham, MA, USA), and 750 ng of autoclaved salmon sperm DNA. The mixture was added to a slide and covered with a 22 × 22 mm plastic cover slip. Slides were placed in a metal tray floating in boiling water bath for 4 min to denature the probe and chromosomal DNA as described by Kato et al. (2004, 2006) and transferred to a 55 °C oven for overnight hybridization. Slides were washed in 2 × SSC buffer for 5 min at room temperature and 20 min at 55 °C. Chromosome preparations were mounted and counterstained with 4′,6- diamidino-2-phenylindole (DAPI) in Vectashield (Vector Laboratories, Burlingame, CA, USA).

Images were captured using a Zeiss AxioImager M2 microscope with a Zeiss Axiocam 506, Zeiss AxioVision SE64 Rel. 4.9.1 software and processed using the Adobe Photoshop software (Adobe Systems Incorporated, San Jose, CA, USA).

DNA marker analysis

Wheat genomic DNA was extracted from young leaves as described by Niu et al. (2011). The wheat 90 K iSelect single nucleotide polymorphism (SNP) arrays (Wang et al. 2014) were used to genotype the recombinants and their parents. The genotype calling and allele clustering were performed using GenomeStudio 2.0 (Illumina, Inc.). Polymerase chain reaction (PCR) for the Sequence-Tagged Sites (STS) markers was conducted in a 20-µl reaction mixture with 100 ng DNA template using GoTaq Green Master Mix (Promega, USA). The thermal cycler conditions were set as: one cycle of 94 °C for 3 min, 35 cycles of denaturing for 30 s at 94 °C, annealing for 40 s at 57 °C, and extension for 60 s at 72 °C, and one cycle of 72 °C for 5 min. The gel images were captured by AlphaImager® Gel Documentation System (Protein Simple Inc., Santa Clara, California, USA) under UV light exposure.

The semi-thermal asymmetric reverse PCR (STARP) marker was developed and run as described by Long et al. (2017). The STARP amplicons were separated by IR2 4200 DNA Analyzer with denaturing polyacrylamide gel electrophoresis (LI-COR, Lincoln, NE, USA) (Long et al. 2017; Zhang et al. 2017).

Fhb7 resides at the terminal region of the long arm of *Thinopyrum* chromosome 7E (Wang et al. 2020). We used the coding sequence tplb0007o14 physically mapped to the terminal regions on the long arms of wheat group-7 chromosomes (Danilova et al. 2017) as an anchor point to develop a SNP-based PCR Allelic Competitive Extension (PACE) marker diagnostic for the 7EL segment harboring *Fhb7*. SNP search was performed within the targeted regions by aligning the group-7 homoeologous sequences of *T. aestivum*, *T. turgidum*, *T. urartu*, and *Ae. tauschii* from the IWGSC data repository (Alaux et al., 2018) and those from *Th. elongatum* Sequence Read Archive (SRA) reads SRR1609124 using the NCBI BLAST (Altschul et al. 1990). The E- and B-genome specific SNPs were used to design shifted PACE markers (Danilova et al. 2019). PACE reaction mixture (3CR Bioscience Ltd, Welwyn Garden City, UK) and PCR conditions were as described by Danilova et al. (2019). Primers were synthesized by Integrated DNA Technologies, Inc. (Coralville, IA, USA). The PCR results were read using a Bio-Rad CFX96 machine (Bio-Rad Laboratories, Inc., Hercules, CA, USA).

Fhb7 variant cloning and sequence analysis

The STS primer pairs of *Xwgc2316* were designed based on the BAC clone *NODE_28_length_58203_cov_9148.280322*, which spans the *Fhb7* locus (Wang et al. 2020). They were used to amplify the *Fhb7* allele, from the FHB-resistant 7B–7E recombinant produced from DS 7E(7B). The STS amplicons were purified using QIAquick Gel Extraction Kit (Qiagen, USA) and then sequenced by GenScript, Inc., USA. The DNA and the amino acid sequences of the *Fhb7* alleles involved in this study were aligned to each other by MulTAlin (Corpet 1988). The protein structures conditioned by the *Fhb7* alleles were predicted using the SWISS-MODEL (https://swissmodel.expasy.org/interactive).

Flour color and yellow pigment analysis

Wheat kernels were first cleaned using a Carter-Day dockage tester (Carter Day International, Minneapolis, MN) to remove untargeted material and broken kernels. Wheat samples (100 g) were conditioned to 16% moisture content prior to being milled on a Brabender Quadrumat Jr. mill (C.W. Brabender Instruments, Inc., South Hackensack, NJ) according to AACCI Method 26-50.01 (2010). Flour fractions were collected and analyzed for color and yellow pigment determinations.

Flour color was measured using a Minolta CR-410 Chroma Meter equipped with a CR-A50 granular material

attachment (Konica Minolta Sensing Americas, Inc., Ramsey, NJ). Values are expressed as Commission Internationale de l'Éclairage, L^*, a^*, and b^* (CIELAB 1986) where L^* represents lightness (0 = black; 100 = white), while a^* and b^* represent redness (− a* = greenness) and yellowness (− b* = blueness), respectively.

Yellow pigment concentration was determined according to AACCI Method 14-60.01 (2012) with some modifications. Flour samples (2 g) were extracted in 10 mL of water-saturated butanol (WSB) for 5 min using a vortex mixer set at medium–high speed and were then rested at room temperature in the absence of light for 1 h. The mixtures were then vortexed for another 5 min and left to rest as stated above for 18 h. After the resting period, the extracts were centrifuged for 10 min at 4,000 g. The supernatants were decanted, and their absorptions were measured at 450 nm. Yellow pigment concentration was calculated using the measured absorption and the absorption coefficient ($A^{1\%}$) of lutein in WSB ($A^{1\%} = 2474$). Yellow pigment concentrations are expressed as µg lutein equivalents/g.

Results

Molecular cytogenetic characterization and isolation of the 7B–7E recombinants critical for the *Fhb7* locus

The *Fhb7* locus resides in the distal region of the long arm of *Th. elongatum*/*Th. ponticum* chromosome 7E (7EL) (Guo et al. 2015; Wang et al. 2020). In this study, we selected a double crossover-derived 7B–7E recombinant involving the terminal regions of 7BL and 7EL (i.e., 7BS·7BL–7EL–7BL) that likely contained the *Fhb7* locus on the smallest 7EL segment in our 7B–7E recombinant pool (Zhang et al. 2020) for further cytogenetic and genomic characterization of the *Fhb7* locus. This recombinant was initially recovered from a 7B–7E recombination population using wheat 90 K SNP arrays. The 7BL terminal segment on the recombinant chromosome was not detected by genomic in situ hybridization (GISH) in the previous study of Zhang et al. (2020). Here, we performed a multi-probe (or called multi-color) FISH analysis of the original 7B–7E recombinant line and found that it was a mixture of two recombinants, including a double crossover-derived recombinant (7BS·7BL–7EL–7BL) and a single crossover-derived recombinant (7BS·7BL–7EL). The recombinants 7BS·7BL–7EL–7BL and 7BS·7BL–7EL were individually isolated from the original recombinant line and hereafter are designated WGC001 and WGC002, respectively (Figs. 1 and S1).

Three FISH probes, including E genome-specific repeats, (GAA)n, and pSc119.2, generated diagnostic patterns in the terminal regions of chromosomes 7B in CS and 7E in DS 7E(7B). pSc119.2 (labeled red) detected a terminal segment on 7EL, but not on 7BL. This clearly differentiated 7BS·7BL–7EL from 7BS·7BL–7EL–7BL. Also, a small terminal segment of 7BL was directly visualized in 7BS·7BL–7EL–7BL by the multi-color FISH (Figs. 1 and S1).

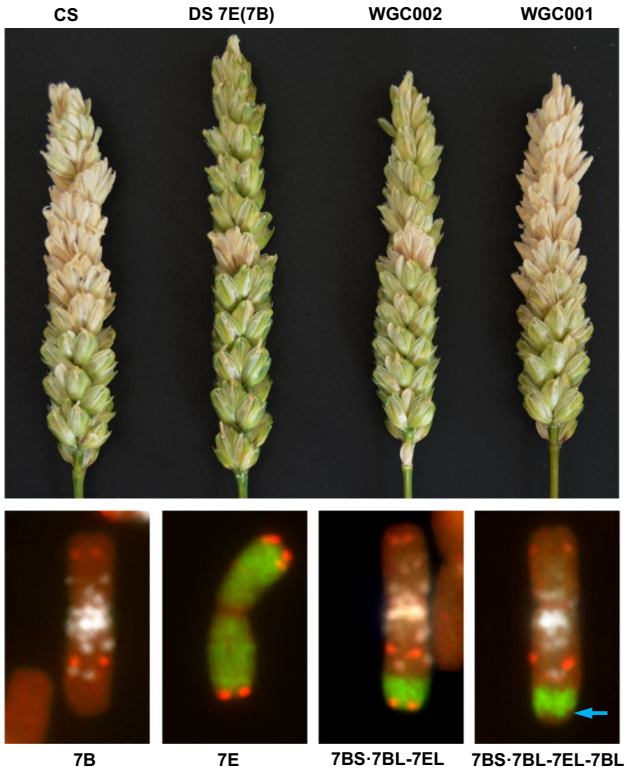

Fig. 1 Reactions of CS, DS 7E(7B), and 7B-7E translocation lines to FHB infection (*top*) and FISH patterns of CS chromosome 7B, *Th. elongatum* chromosome 7E, and two 7B–7E translocated chromosomes (*bottom*). *Th. elongatum* chromatin, (GAA)n repeat, and pSc119.2 repeat are painted green, white, and red, respectively. Chromosomes counterstained with DAPI are shown in orange pseudocolor. Arrow points to the terminal 7BL segment (orange-counterstain) that replaced the 7EL segment (red-pSc119.2 repeat at the end) containing *Fhb7*^{The2} on the translocated chromosome 7BS·7BL–7EL–7BL

Reaction of the 7B–7E recombinants WGC001 and WGC002 to FHB

The 7B–7E recombinants WGC001 (7BS·7BL–7EL–7BL) and WGC002 (7BS·7BL–7EL) were evaluated for FHB resistance with four replications in 1–3 greenhouse seasons. DS 7E(7B) and its wheat parent 'CS' were used as resistant and susceptible controls, respectively, in the FHB evaluation experiments. WGC002 consistently exhibited an FHB severity similar to DS 7E(7B), which was significantly lower than CS in all three screening seasons. WGC001, however, showed an FHB severity equivalent to CS, which was

significantly higher than DS 7E(7B) and WGC002 (Table 1 and Fig. 1). The reaction of these two 7B–7E recombinants and their parents to FHB indicated that *Th. elongatum* chromosome 7E in DS 7E(7B) and the terminal 7EL segment in WGC002 contained the gene for FHB resistance, whereas the 7EL segment in WGC001 lost the resistance gene due to the small 7BL–7EL recombination within the terminal regions (Fig. 1). Thus, the recombinants 7BS·7BL–7EL and 7BS·7BL–7EL–7BL resolved the position of the FHB resistance locus on 7EL and were critical for genomic analysis of the resistance gene.

Genomic analysis of the *Fhb7* locus in the critical 7B–7E recombinants

The *Th. ponticum*-derived *Fhb7* cloned by Wang et al. (2020), here designated $Fhb7^{Thp}$, encompasses a genomic segment of 846 bp in the distal region of 7EL. Meanwhile, the *Fhb7* allele was identified within the same chromosomal region (739,934,264 bp–739,935,109 bp) from the reference E genome of *Th. elongatum* (Wang et al. 2020), which is designated $Fhb7^{The1}$ in this study. We developed an *Fhb7*-specific STS marker (*Xwgc2315*) (Fig. 2b and Table 2) based on the genomic sequence of $Fhb7^{Thp}$ (Wang et al. 2020) and used *Xwgc2315* to examine the presence of the *Fhb7* locus in the recombinants 7BS·7BL–7EL and 7BS·7BL–7EL–7BL. We found that the *Fhb7* locus was present in 7BS·7BL–7EL, but not in 7BS·7BL–7EL–7BL, which was consistent with their responses to FHB. Therefore, the terminal 7EL segment replaced by the homoeologous counterpart of 7BL in 7BS·7BL–7EL–7BL contains the *Fhb7* locus with an FHB-resistant allele hereby designated $Fhb7^{The2}$ (Fig. 2a and b).

We positioned the homoeologous recombination breakpoints in the recombinant chromosomes 7BS·7BL–7EL and 7BS·7BL–7EL–7BL using wheat 90 K SNP arrays (Table S1 and Fig. 2). Initially, the wheat 90 K SNPs were aligned to chromosome 7B using IWGSC RefSeq v2.0 (Table S1). The sizes of the alien introgression segment and the position of $Fhb7^{The2}$ in the recombinant chromosomes were determined using the recent IWGSC RefSeq v2.1 (Zhu et al. 2021) and *Th. elongatum* 7E sequence (GenBank accession CM022303.1; Wang et al. 2020). The full lengths of chromosomes 7B and 7E were determined as 764,081,788 bp and 744,091,923 bp, respectively, according to IWGSC RefSeq v2.1 and CM022303.1. The primary 7EL–7BL recombination breakpoint mapped between SNPs *IWB58112* (656,740,791 bp) and *IWB31227* (661,206,798 bp) on wheat chromosome 7B. The size of the distal 7BL segment, substituted by 7EL chromatin in the recombinant chromosome 7BS·7BL–7EL of WGC002, was estimated to be ~ 105 Mbp. Both *IWB31227* and *IWB9204* were absent on chromosome 7E. So, the primary 7BL–7EL recombination breakpoint in the recombinant 7BS·7BL–7EL mapped to the midpoint between *IWB58112* (656,740,791 bp) and *IWB75604* (635,440,226 bp) (Fig. 2a). As a result, the physical size of the 7EL segment in 7BS·7BL–7EL was estimated as ~ 111 Mbp. The distal secondary 7EL–7BL recombination breakpoint in the recombinant 7BS·7BL–7EL–7BL of WGC001 was positioned to the interval flanked by the SNPs *IWB55488* (744,248,183 bp) and *IWB49181* (745,376,542 bp) on wheat chromosome 7B. The terminal 7BL segment that replaced its homoeologous counterpart of 7EL containing $Fhb7^{The2}$ in 7BS·7BL–7EL–7BL was estimated to be approximately 19 Mbp in length according to the IWGSC RefSeq v2.1 assembly (Zhu et al. 2021). The terminal 7EL segment containing $Fhb7^{The2}$, which was replaced by its homoeologous 7BL counterpart in the recombinant 7BS·7BL–7EL–7BL of WGC001, was estimated as ~ 30 Mbp based on the wheat 90 K SNP genotyping data and the reference genome sequences of chromosome 7E (Wang et al. 2020) (Fig. 2a).

In addition, we developed a SNP-based co-dominant PACE marker (*Xwgc2317*) that was diagnostic for the 7EL distal region (~ 30Mbp) containing $Fhb7^{The2}$ (Table 2; Figs. 2a and 2c). The homoeoallele of *Xwgc2317* on 7BL was located at 754,117,575 bp (Fig. 2a). It is a user-friendly SNP-based marker useful for high-throughput marker-assisted selection (MAS) of $Fhb7^{The2}$ in wheat breeding.

Cloning of $Fhb7^{The2}$ and comparative analysis of $Fhb7^{The2}$ with $Fhb7^{Thp}$ and $Fhb7.^{The1}$

The *Fhb7* locus has been reported to be horizontally transferred to the E genome of *Thinopyrum* species from fungus *Epichloë aotearoae*. A unique *E. aotearoae*-originated fragment harboring the *Fhb7* locus has been identified in

Table 1 FHB severity of CS, DS 7E(7B), and 7B–7E translocation lines

Genotypes	Chromosome constitution	Mean FHB severity (%)		
		2019 fall	2021 spring	2021 summer
T. aestivum 'CS'	21″ (CS)	49.17 ± 7.54a*	58.64 ± 12.33a	62.82 ± 9.33a
DS 7E(7B)	20″ (CS) + 1″7E(7B)	6.97 ± 3.22b	10.36 ± 5.84b	6.94 ± 3.12b
WGC002	20″ (CS) + 1″T7BS·7BL-7EL	6.42 ± 1.31b	10.17 ± 5.89b	6.78 ± 2.95b
WGC001	20″ (CS) + 1″T7BS·7BL-7EL-7BL	–	–	58.16 ± 10.78a

*Mean ± standard deviation, values followed by different letters are significantly different at $p = 0.05$ level

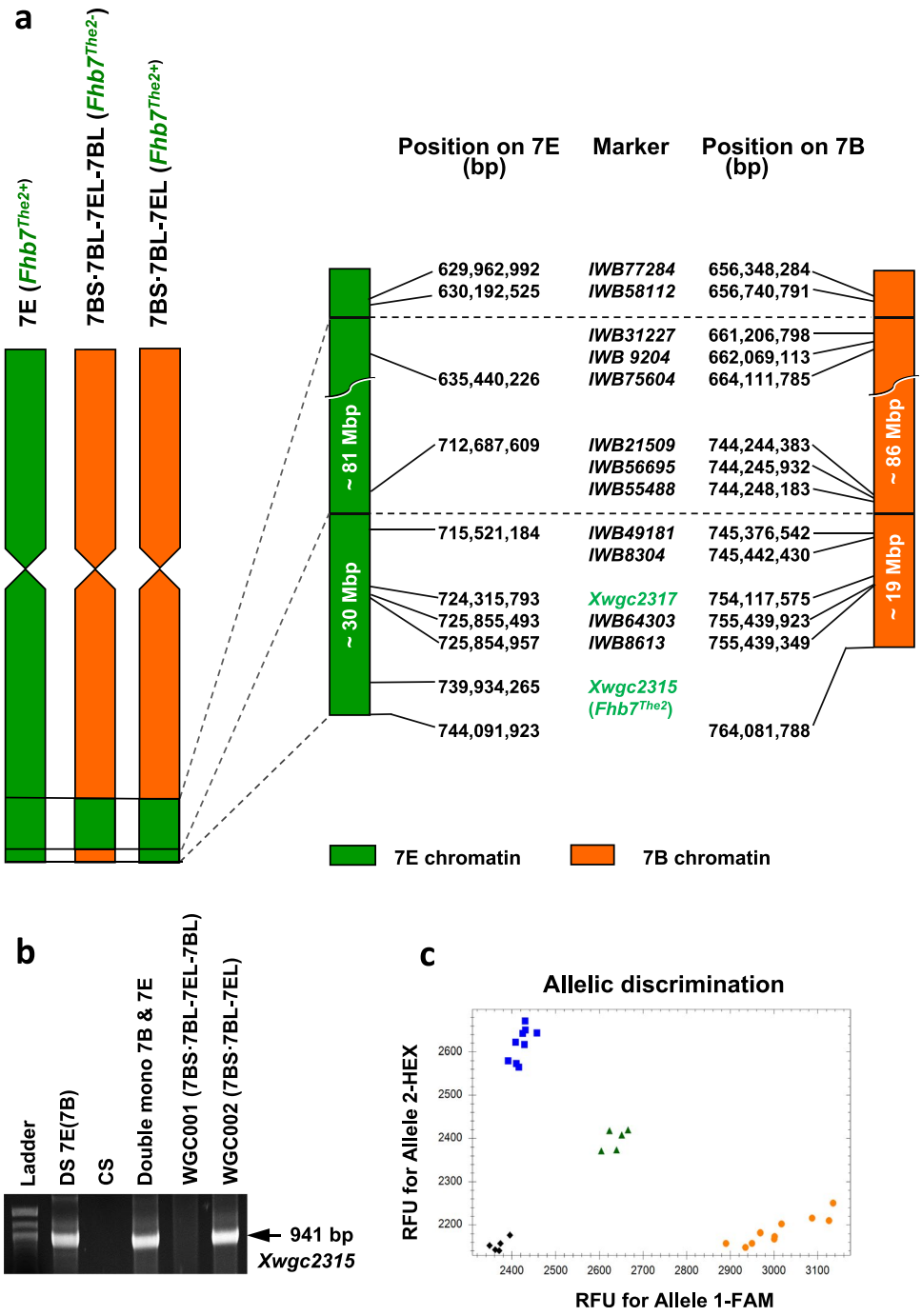

Fig. 2 Physical mapping and molecular marker analysis of the 7B–7E recombinants and *Fhb7*^{The2}. **a** Physical maps of the recombinants 7BS·7BL–7EL and 7BS·7BL–7EL–7BL. **b** *Fhb7*^{The2}-specific molecular marker analysis with STS *Xwgc2315*; and **c** PACE genotyping assay with co-dominant SNP marker *Xwgc2317*. Individuals homozygous for the wheat 7B alleles (CS and WGC001) at the *Xwgc2317* locus are showed as blue squares, heterozygous for the 7B and 7E alleles as green triangles, and homozygous for the 7E allele [DS7E(7B) and WGC002] as yellow circles (color figure online)

the reference E genome (Wang et al. 2020). Based on the genomic sequences flanking the *E. aotearoae*-originated fragment in the reference E genome, we designed an STS (*Xwgc2316*) primer pair (Table 2) to amplify the fragment including the *Fhb7*^{The2} allele from the 7EL segment in the FHB-resistant recombinant WGC002. DNA sequence analysis of the amplicons identified the coding sequence of 846 bp for *Fhb7*^{The2}. In addition, we recovered 32 bp upstream and 19 bp downstream *E. aotearoae*-derived sequences flanking the *Fhb7*^{The2} allele.

A total of 12 SNPs were identified in the coding regions of the *Fhb7* alleles *Fhb7*^{Thp}, *Fhb7*^{The1}, and *Fhb7*^{The2} (Figs. 3 and S1). Seven of the SNPs lead to amino acid changes in translation. Out of the seven SNP-derived amino acid changes, two are nonpolar-to-polar uncharged conversions (*A5T* and *P128Q*) and one basic-to-polar uncharged conversion (*R220Q*). The other four SNPs cause amino acid that do not alter chemical properties of amino acid. No DNA sequence variation was detected in the 32 bp upstream and 19 bp downstream *E.*

Table 2 Primer sequences and amplicons of the STS, PACE, and STARP markers specific for *Fhb7*^{The} and *PSY-E1*

Marker	Type	Primers	Sequence (5′–3′)[a]	Amplicon size
Xwgc2315	STS	Forward	AGCTTCAGTCAACCCTTTTCT	941 bp
		Reverse	CTTCATCTCCGAGACCTAGC	
Xwgc2316	STS	Forward	AGCTTCAGTCAACCCTTTTCT	961 bp
		Reverse	AGCTACTTCACCTCGGCA	
Xwgc2317	PACE	Forward 7B	FAM-TATCTTGTCCTGTTGACCTCCC	95 bp
		Forward 7E	HEX-TATCTTATCCTGTTGACCTCCTGC	
		Reverse	GACAGTCCATTTACGGTGCTTT	
		Forward1	[Tail1]-TGTAGCTAGAGGGATCGAG	
Rwgsnp41	STARP	Forward2	[Tail2]-TGTAGAGGGATCGAGCCAT	93/97 bp
		Reverse	TCGGCCACTCACCTCTTATC	

a [Tail1] = GCAACAGGAACCAGCTATGAC; [Tail2] = GACGCAAGTGAGCAGTATGAC

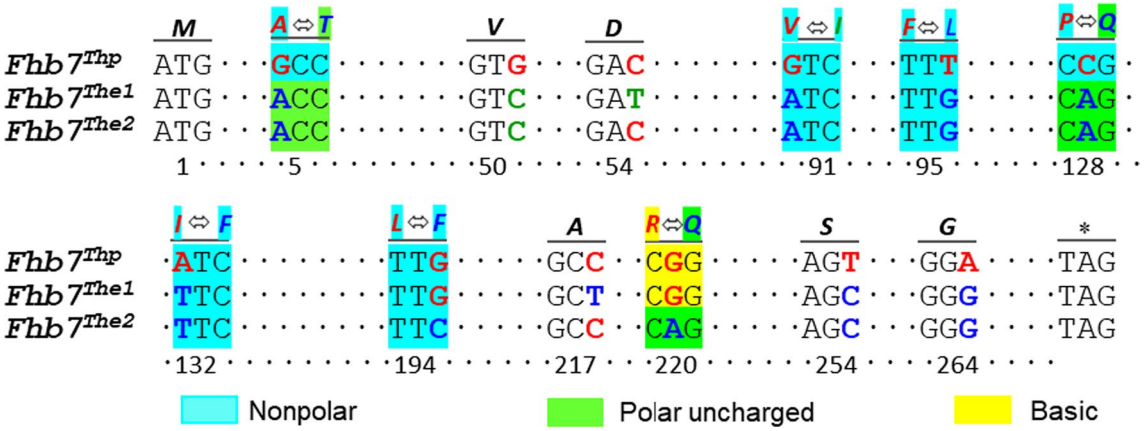

Fig. 3 Variation of *Fhb7*^{Thp}, *Fhb7*^{The1}, and *Fhb7*^{The2} in their coding DNA sequences and encoded amino acids. The italic letters above the solid lines in the top rows are the letter codes of the amino acids specified by the corresponding codons with SNPs. Codons specify nonpolar, polar uncharged, and basic amino acids are highlighted in light blue, green, and yellow, respectively. The numbers at the bottom indicate the positions of the codons in the coding sequences (color figure online)

aotearoae-derived sequences flanking these three *Fhb7* alleles.

The amino acid sequences of Fhb7^{Thp}, Fhb7^{The1}, and Fhb7^{The2} were used as queries to search against the SWISS-MODEL database (https://swissmodel.expasy.org/interactive). The glutathione transferase GSTFuA3 from *Phanerochaete chrysosporium* was found to be the best template to build structural models for the three variants. The predicted ribbon models of Fhb7^{Thp}, Fhb7^{The1}, and Fhb7^{The2} were highly similar to each other with 28.7%, 29.1%, and 28.9% of identities to the crystal structure of glutathione transferase GSTFuA3, respectively (Figure S3).

Flour color determination of the FHB-resistant 7B–7E translocation line and genomic analysis of the yellow pigment gene *PSY-E1* closely linked to *Fhb7*

Both DS 7E(7B) and WGC002 showed a *b** value (yellowness) similar to their wheat parent 'CS', indicating a low level of yellow pigment in the flour. In addition, the flour of DS 7E(7B) and WGC002 had a high *L** value for lightness (over 90 in a 0–100 lightness scale), equivalent to CS. The flour carotenoid content of DS 7E(7B) and WGC002 fell in the normal range of wheat flours (Table 3). Apparently, the

Table 3 Flour pigment testing of CS, DS 7E(7B), and FHB-resistant 7B-7E translocation line WGC002

Sample	Flour color[a]			Total carotenoid content[b](µg lutein equiv./g)
	*L**	*a**	*b**	
CS	91.15	−0.74	8.86	2.03
DS 7E(7B)	91.59	−0.75	7.96	1.41
WGC002	90.55	−0.53	9.55	2.30

[a]Flour color determination using the colorimeter: *L** Lightness measurement of the flour on a scale of 0 (black) to 100 (white); *a** Redness (−***a****=greenness); *b** Yellowness (−*b**=blueness)

[b]Total carotenoid content determined using UV/Vis spectrophotometer

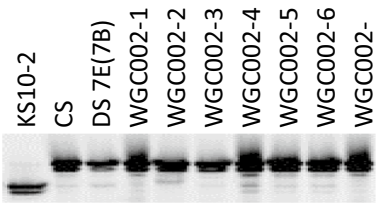

Fig. 4 Gel electrophoresis image of the STARP marker *Rwgsnp41* in KS10-2 (positive control for the yellow flour pigment gene *PSY-E1*), CS [wheat parent for DS 7E(7B) and WGC002], DS 7E(7B), and seven individuals of the FHB-resistant translocation line WGC002 containing *Fhb7* on the CS-*Th. elongatum* translocation chromosome 7BS·7BL–7EL. The lower band is specific for *PSY-E1* on *Th. ponticum* chromosome arm $7el_2L$ and upper band for the homoeoallele of *PSY-E1* on wheat chromosome 7DL

Th. elongatum chromosome 7E in DS 7E(7B) and the distal segment of 7EL in WGC002 do not contain the *PSY-E1* gene for yellow flour pigment as reported on *Th. ponticum* chromosome 7E (Zhang and Dubcovsky 2008; Zhang et al. 2005).

The STARP marker *Rwgsnp41* was developed specifically for the yellow flour pigment gene *PSY-E1* on *Th. ponticum* chromosome arm $7el_2L$ and for the homoeoallele of *PSY-E1* on wheat chromosome 7D based on the DNA sequence of *PSY-E1* reported by Zhang and Dubcovsky (2008) and group 7 DNA sequences in IWGSC RefSeq v2.1 (https://urgi.versailles.inrae.fr/blast_iwgsc/?dbgroup=wheat_iwgsc_refseq_v2.1_chromosomes&program=blastn). *Rwgsnp41* was used to determine whether *PSY-E1* was present or absent on the *Th. elongatum* chromosome 7E involved in DS 7E(7B) and WGC002. A unique allele was identified at the *PSY-E1* locus in KS10-2 ($7DS\text{-}7el_2S{\cdot}7el_2L$) that contains the wild type of *PSY-E1* allele for yellow flour on *Th. ponticum* chromosome arm $7el_2L$. A homoeoallele of *PSY-E1* was detected on chromosome 7D of CS, DS 7E(7B), and the FHB resistance line WGC002 containing *Fhb7* (Fig. 4). Thus, the *Th. elongatum* chromosome 7E in DS 7E(7B) and the translocated chromosome 7BS·7BL–7EL in WGC002 contain $Fhb7^{The2}$ for FHB resistance, but not *PSY-E1* for yellow flour. Both flour pigment and genomic analysis consistently indicate that the *PSY-E1* allele in KS10-2 conditions yellow flour, while DS 7E(7B) and WGC002 do not have the same allele for yellow flour. Hence, the 7B–7E translocation line WGC002 can be utilized directly in wheat breeding for FHB resistance without the unwanted linkage drag associated with yellow flour pigmentation.

Discussion

Fhb7 was derived from tall wheatgrass, including diploid *Th. elongatum* and decaploid *Th. ponticum* that shares the E genome of *Th. elongatum*. It resides in the very terminal region of 7EL (Fig. 2 and Wang et al. 2020). The physical location of *Fhb7* dramatically facilitated the success of its introgression from 7E to 7B by meiotic homoeologous recombination in this study, making this wild species-derived FHB resistance gene usable directly in wheat breeding programs without obvious linkage drag. Furthermore, the *Th. elongatum* chromosome 7E-derived FHB resistance allele $Fhb7^{The2}$ has been incorporated into the wheat B genome by 7B–7E translocation. This has made $Fhb7^{The2}$ available for FHB-resistant variety development in both common and durum wheat that share the B genome. The other *Fhb7* introgression lines involving wheat chromosome 7D (Guo et al. 2015; Fedak et al. 2021; Ceoloni et al. 2017) are limited for use in hexaploid common wheat breeding programs due to the presence of the yellow flour pigment gene closely linked to that *Fhb7* allele and have no utility in durum wheat breeding programs because of the absence of D genome in tetraploid durum.

The yellow flour pigment gene *PSY-E1* is very closely linked to the $Fhb7^{Thp}$ allele. The physical distance between these two genes is approximately 18 Mbp (Zhang and Dubcovsky 2008; Wang et al. 2020). It has been a big challenge for multiple research groups to break the tight linkage over the years. This has limited the utilization of $Fhb7^{Thp}$ and other disease resistance genes within the genomic region (Zhang et al. 2005; Niu et al. 2014) in wheat breeding program, especially in common wheat where yellow flour pigmentation is not a desirable end-use quality trait. In this study, we found that the FHB-resistant 7B–7E translocation line containing $Fhb7^{The2}$ produced regular white flours as its wheat parent. There is no yellow flour linkage drag associated with $Fhb7^{The2}$, which makes this FHB-resistant introgression line immediately usable in wheat breeding programs. The marker analysis in this study indicated the *Th. elongatum* chromosome 7E containing $Fhb7^{The2}$ might have a variant allele of *PSY-E1* that does not condition yellow pigment in the flour. This result demonstrates the novelty of

Fhb7^{The2} by having a unique haplotype within the genomic region.

Fhb7^{The2} has been integrated into wheat chromosome 7B through a small 7B–7E translocation (7BS·7BL–7EL) in this study. The integrative cytogenetic and genomic analysis of two critical 7B–7E recombinant chromosomes (7BS·7BL–7EL and 7BS·7BL–7EL–7BL) delimited *Fhb7*^{The2} to a genomic region of about 30 Mbp at the end of 7EL, which corresponds to a homoeologous region of ~ 19 Mbp on 7BL. The 7EL segment in the FHB-resistant recombinant 7BS·7BL–7EL was estimated at ~ 111 Mbp in length, which is equivalent to its homoeologous counterpart of ~ 105 Mbp on 7BL. Obvious deleterious linkage drag has not been observed with the FHB-resistant recombinant line WGC002 (7BS·7BL–7EL). In addition, the 7EL segment containing *Fhb7*^{The2} in 7BS·7BL–7EL exhibits a monogenic inheritance pattern in the wheat genetic background. User-friendly and diagnostic DNA markers were developed specifically for *Fhb7*^{The2} and the 7EL segment containing *Fhb7*^{The2}. They will be extremely useful for the selection of *Fhb7*^{The2} in FHB resistance introgression and breeding. In contrast to other complex FHB resistance QTL, the wild species-derived resistance genes like *Fhb7*^{The2} exhibit advantages in the efficacy of marker-assisted selection in FHB resistance introgression, pyramiding, and variety development because of the nature of their monogenic inheritance. We have been using these markers to deploy *Fhb7*^{The2} in both common and durum wheat varieties.

The diploid *Th. elongatum*-derived *Fhb7* allele *Fhb7*^{The2} conditioned FHB resistance in the wheat genetic background as the decaploid *Th. ponticum*-derived *Fhb7* allele *Fhb7*^{Thp} (Wang et al. 2020). *Fhb7*^{The1}, which was identified directly from a *Th. elongatum* accession, was also reported to confer resistance reaction to FHB infection. We found that these three *Fhb7* alleles differed at 12 SNPs in their coding regions, which led to seven amino acid conversions. However, Fhb7^{Thp}, Fhb7^{The1}, and Fhb7^{The2} were predicted to have a similar functional configuration as a glutathione transferase in this study. This was probably why they exhibited similar reactions to FHB infection. Both diploid *Th. elongatum* and decaploid *Th. ponticum* are mostly cross-pollinated and highly heterogeneous perennial grass species. *Fhb7* has probably undergone various structural alterations upon integration into the *Th. elongatum*/*Th. ponticum* genomes from the fungus (Wang et al, 2020). However, its function as a resistance gene to FHB appears to be preserved over the evolutionary lineage of tall wheatgrass due probably to the constant disease pressure posed by the FHB pathogen.

In summary, we identified and integrated a novel *Th. elongatum*-derived *Fhb7* resistance allele (*Fhb7*^{The2}) into the wheat B genome through meiotic homoeologous recombination-base chromosome engineering, making this FHB resistance gene immediately usable in the variety and germplasm development of both common and durum wheat. No obvious linkage drag has been observed with *Fhb7*^{The2} in the FHB-resistant introgression line we developed. The user-friendly and diagnostic DNA markers we developed specifically for *Fhb7*^{The2} and the 7EL segment containing *Fhb7*^{The2} will further enhance the utility of this unique resistance source in wheat breeding and related genetic studies.

Supplementary Information The online version contains supplementary material available at https://doi.org/10.1007/s00122-022-04228-3.

Acknowledgements We thank Mary Osenga for her assistance in high-throughput SNP genotyping.

Author contributions statement WZ contributed to marker development and analysis, cloning, recombinant production and analysis, and data preparation and analysis. TD performed FISH/GISH analysis, SNP marker development, and involved in manuscript preparation. MZ contributed to recombinant production and analysis and SNP assays. SR performed FHB disease evaluation. XZ participated in crossing and chromosome-specific marker analysis for recombinant production. QZ was involved in DNA marker development. SZ was involved in FHB disease evaluation. L.D. performed flour color analysis and contributed to manuscript preparation. JF contributed SNP assays. SX contributed to experiment planning, interpretation, and manuscript preparation. KF contributed to experimental results interpretation and critical revision of the manuscript. SW contributed to FHB disease evaluation and manuscript preparation. JB: contributed to the DNA marker development and critical revision of the manuscript. XC designed and coordinated this work, and was involved in crosses, data analysis and interpretation, and led the manuscript preparation.

Funding This project has been supported by Agriculture and Food Research Initiative Competitive Grant no. 2013-67013-21121 and 2019-67013-35750 from the USDA National Institute of Food and Agriculture, and the US Wheat & Barley Scab Initiative Grant no. 59-0206-7-002.

Data availability The datasets generated during and/or analyzed during the current study are available from the corresponding author on reasonable request.

Declarations

Conflict of interest The authors declare that they have no conflict of interest. The authors have no relevant financial or non-financial interest to disclose.

References

AACCI (2010) Approved methods of analysis, 26-50.01. Brabender Quadrumat Jr. (Quadruplex) method. Cereals & grains association, St. Paul, MN, USA. https://doi.org/10.1094/AACCIntMethod-26-50.01

AACCI (2012) Approved methods of analysis, 14-60.01. Total carotenoid content of cereal grains and flours. Cereals & grains association, St. Paul, MN, USA. https://www.cerealsgrains.org/resources/Methods/Methods/14-60.pdf

Alaux M, Rogers J, Letellier T, Flores R, Alfama F, Pommier C, Mohellibi N, Durand S, Kimmel E, Michotey C et al (2018) Linking the international wheat genome sequencing consortium bread

wheat reference genome sequence to wheat genetic and phenomic data. Genome Biol 19:111
Altschul SF, Gish W, Miller W, Myers EW, Lipman DJ (1990) Basic local alignment search tool. J Mol Biol 215:403–410
Buerstmayr H, Stierschneider M, Steiner B, Lemmens M, Griesser M, Nevo E, Fahima T (2003) Variation for resistance to head blight caused by *F. graminearum* in wild emmer originating from Israel. Euphytica 130:17–23
Cai X, Chen PD, Xu SS, Oliver RE, Chen X (2005) Utilization of alien genes to enhance Fusarium head blight resistance in wheat: a review. Euphytica 142:309–318
Cainong JC, Bockus WW, Feng Y, Chen P, Qi L, Sehgal SK, Danilova TV, Koo D-H, Friebe B, Gill BS (2015) Chromosome engineering, mapping, and transferring of resistance to Fusarium head blight disease from *Elymus tsukushiensis* into wheat. Theor Appl Genet 128:1019–1027
Ceoloni C, Forte P, Kuzmanovic L, Tundo S, Moscetti I, De Vita P, Virili ME, D'Ovidio R (2017) Cytogenetic mapping of a major locus for resistance to Fusarium head blight and crown rot of wheat on *Thinopyrum elongatum* 7EL and its pyramiding with valuable genes from a *Th. ponticum* homoeologous arm onto bread wheat 7DL. Theor Appl Genet 130:2005–2024
Chen X, Faris J, Hu J, Stack R, Adhikari T, Elias E, Kianian S, Cai X (2007) Saturation and comparative mapping of a major Fusarium head blight resistance QTL in tetraploid wheat. Mol Breed 19:113–124
CIE (1986) Colorimetry (Publication 15.2), 2nd edn. Commission Internationale de L'Éclairage, Vienna, Austria
Corpet F (1988) Multiple sequence alignment with hierarchical clustering. Nucl Acids Res 16(22):10881–10890
Danilova TV, Friebe B, Gill BS (2012) Single-copy gene fluorescence in situ hybridization and genome analysis: Acc-2 loci mark evolutionary chromosomal rearrangements in wheat. Chromosoma 121:597–611
Danilova TV, Poland J, Friebe B (2019) Production of a complete set of wheat–barley group-7 chromosome recombinants with increased grain β-glucan content. Theor Appl Genet 132:3129–3141. https://doi.org/10.1007/s00122-019-03411-3
Danilova TV, Akhunova AR, Akhunov ED, Friebe B, Gill BS (2017) Major structural genomic alterations can be associated with hybrid speciation in *Aegilops markgrafii* (Triticeae). Plant J 92:317–330
Fedak G, Chi D, Wolfe D, Ouellet T, Cao WG, Han FP, Xue A (2021) Transfer of fusarium head blight resistance from *Thinopyrum elongatum* to bread wheat cultivar Chinese spring. Genome 64:997–1008
Forte P, Virili ME, Kuzmanović L, Moscetti I, Andrea Gennaro A, D'Ovidio R, Ceoloni C (2014) A novel assembly of *Thinopyrum ponticum* genes into the durum wheat genome: pyramiding Fusarium head blight resistance onto recombinant lines previously engineered for other beneficial traits from the same alien species. Mol Breed 34:1701–1716
Grewal S, Hubbart-Edwards S, Yang C, Devi U, Baker L, Heath J, Scholefield SAD, Howells C, Yarde J, Isaac P, King IP, King J (2020) Rapid identification of homozygosity and site of wild relative introgressions in wheat through chromosome-specific KASP genotyping assays. Plant Biotechnol J 18:743–755
Guo J, Zhang X, Hou Y, Cai J, Shen X, Zhou T, Xu H, Ohm HW, Wang H, Li A, Han F, Wang H, Kong L (2015) High-density mapping of the major FHB resistance gene Fhb7 derived from *Thinopyrum ponticum* and its pyramiding with Fhb1 by marker-assisted selection. Theor Appl Genet 128:2301–2316
Haile JK, N'Diaye A, Walkowiak S, Nilsen KT, Clarke JM, Kutcher HR, Steiner B, Buerstmayr H, Pozniak CJ (2019) Fusarium head blight in durum wheat: recent status, breeding directions and future prospects. Phytopathology 109:1664–1675
Kato A, Lamb JC, Birchler JA (2004) Chromosome painting using repetitive DNA sequences as probes for somatic chromosome identification in maize. Proc Natl Acad Sci USA 101:13554–13559
Kato A, Albert PS, Vega JM, Birchler JA (2006) Sensitive fluorescence in situ hybridization signal detection in maize using directly labeled probes produced by high concentration DNA polymerase nick translation. Biotech Histochem 81:71–78
Kim NS, Armstrong K, Knott DR (1993) Molecular detection of *Lophopyrum* chromatin in wheat–*Lophopyrum* recombinants and their use in the physical mapping of chromosome 7D. Theor Appl Genet 85:561–567
Long Y, Chao WS, Ma G, Xu SS, Qi L (2017) An innovative SNP genotyping method adapting to multiple platforms and throughputs. Theor Appl Genet 130:597–607
McArthur RI, Zhu XW, Oliver RE et al (2012) Homoeology of *Thinopyrum junceum* and *Elymus rectisetus* chromosomes to wheat and disease resistance conferred by the Thinopyrum and Elymus chromosomes in wheat. Chrom Res 20:699–715
McIntyre CL, Pereira S, Moran LB, Appels R (1990) New *Secale cereale* (rye) DNA derivatives for the detection of rye chromosome segments in wheat. Genome 33:635–640
Niu Z, Klindworth DL, Friesen TL, Chao S, Jin Y, Cai X, Xu SS (2011) DNA marker-assisted chromosome engineering of wheat carrying stem rust resistance gene *Sr39* derived from *Aegilops speltoides*. Genetics 187:1011–1021
Niu Z, Klindworth DL, Yu G, Friesen TL, Chao S, Jin Y, Cai X, Ohm J-B, Rasmussen JB, Xu SS (2014) Development and characterization of wheat lines carrying stem rust resistance gene *Sr43* derived from *Thinopyrum ponticum*. Theor Appl Genet 127:969–980
Oliver RE, Stack RW, Miller JD, Cai X (2007) Reaction of wild emmer wheat accessions to Fusarium head blight. Crop Sci 47:893–897
Oliver RE, Cai X, Friesen TL, Halley S, Stack RW, Xu SS (2008) Evaluation of Fusarium head blight resistance in tetraploid wheat (*Triticum turgidum* L.). Crop Sci 48:213–222
Otto CD, Kianian SF, Elias EM, Stack RW, Joppa LR (2002) Genetic dissection of a major Fusarium head blight QTL in tetraploid wheat. Plant Mol Biol 48:625–632
Qi LL, Pumphrey MO, Friebe B, Chen PD, Gill BS (2008) Molecular cytogenetic characterization of alien introgressions with gene *Fhb3* for resistance to Fusarium head blight disease of wheat. Theor Appl Genet 117:1155–1166
Shen X, Kong L, Ohm H (2004) Fusarium head blight resistance in hexaploid wheat (*Triticum aestivum*)-*Lophopyrum* genetic lines and tagging of the alien chromatin by PCR markers. Theor Appl Genet 108:808–813
Szabó-Hevér Á, Zhang Q, Friesen TL, Zhong S, Elias EM, Cai X, Jin Y, Faris JD, Chao S, Xu SS (2018) Genetic diversity and resistance to Fusarium head blight in synthetic hexaploid wheat derived from *Aegilops tauschii* and diverse *Triticum turgidum* subspecies. Front Plant Sci 9:1829
Wang S, Wong D, Forrest K, Allen A, Huang BE, Maccaferri M, Salvi S, Milner SG, Cattivelli L, Mastrangelo AM, Whan A, Stephen S, Barker G, Wieseke R, Plieske J, International Wheat Genome Sequencing Consortium, Lillemo M, Mather D, Appels R, Dolferus R, Brown-Guedira G, Korol A, Akhunova AR, Feuillet C, Salse J, Morgante M, Pozniak C, Luo MC, Dvorak J, Morell M, Dubcovsky J, Ganal M, Tuberosa R, Lawley C, Mikoulitch I, Cavanagh C, Edwards KJ, Hayden M, Akhunov E (2014) Characterization of polyploid wheat genomic diversity using a high-density 90,000 single nucleotide polymorphism array. Plant Biotechnol J 12:787–796
Wang H, Sun S, Ge W, Zhao L, Hou B, Wang K, Lyu Z, Chen L, Xu S, Guo J, Li M, Su P, Li X, Wang G, Bo C, Fang X, Zhuang W, Cheng X, Wu J, Dong L, Chen W, Li W, Xiao G, Zhao J, Hao Y, Xu Y, Gao Y, Liu W, Liu Y, Yin H, Li J, Li X, Zhao Y, Wang X,

Ni F, Ma X, Li A, Xu SS, Bai G, Nevo E, Gao C, Ohm H, Kong L (2020) Horizontal gene transfer of *Fhb7* from fungus underlies Fusarium head blight resistance in wheat. Science 368:eaba5435

Wilson WW, McKee G, Nganje W, Dahl B, Bangsund D (2017) Economic impact of USWBSI's scab initiative to reduce FHB. Agribusiness and applied economics No. 774. North Dakota State Univ

Zhang W, Cai X (2019) Alien introgression and breeding of synthetic wheat. In: Ordon F, Friedt W (eds) Advances in breeding techniques for cereal crops. Burleigh dodds science publishing, Cambridge, pp 3–54

Zhang W, Dubcovsky J (2008) Association between allelic variation at the *Phytoene synthase 1* gene and yellow pigment content in the wheat grain. Theor Appl Genet 116:635–645

Zhang W, Lukaszewski A, Kolmer J, Soria M, Goyal S, Dubcovsky J (2005) Molecular characterization of durum and common wheat recombinant lines carrying leaf rust resistance (*Lr19*) and yellow pigment (*Y*) genes from *Lophopyrum ponticum*. Theor Appl Genet 111:573–582

Zhang X, Shen X, Hao Y, Cai J, Ohm HW, Kong L (2011) A genetic map of *Lophopyrum ponticum* chromosome 7E, harboring resistance genes to Fusarium head blight and leaf rust. Theor Appl Genet 122:263–270

Zhang Q, Axtman JE, Faris JD, Chao S, Zhang Z, Friesen TL, Zhong S, Cai X, Elias EM, Xu SS (2014) Identification and molecular mapping of quantitative trait loci for Fusarium head blight resistance in emmer and durum wheat using a single nucleotide polymorphism-based linkage map. Mol Breed 34:1677–1687

Zhang W, Cao Y, Zhang M, Zhu X, Ren S, Long Y, Gyawali Y, Chao S, Xu S, Cai X (2017) Meiotic homoeologous recombination-based alien gene introgression in the genomics era of wheat. Crop Sci 57:1189–1198

Zhang W, Zhang M, Zhu X, Cao Y, Sun Q, Ma G, Chao S, Yan C, Xu S, Cai X (2018) Molecular cytogenetic and genomic analyses reveal new insights into the origin of the wheat B genome. Theor Appl Genet 131:365–375

Zhang M, Zhang W, Zhu X, Sun Q, Yan C, Xu SS, Fiedler J, Cai X (2020) Dissection and physical mapping of wheat chromosome 7B by inducing meiotic recombination with its homoeologues in *Aegilops speltoides* and *Thinopyrum elongatum*. Theor Appl Genet 133:3455–3467

Zhu X, Zhong S, Chao S, Gu YQ, Kianian SF, Elias E, Cai XW (2016) Toward a better understanding of the genomic region harboring Fusarium head blight resistance QTL *Qfhs.ndsu-3AS* in durum wheat. Theor Appl Genet 129:31–43

Zhu T, Wang L, Rimbert H, Rodriguez JC, Deal KR, De Oliveira R, Choulet F, Keeble-Gagnère G, Tibbits J, Rogers J, Eversole K, Appels R, Gu YQ, Mascher M, Dvorak J, Luo M (2021) Optical maps refine the bread wheat *Triticum aestivum* cv Chinese Spring genome assembly. Plant J 107:303–314